

Assessment of Separation of Functional Components with ICA from Dynamic Cardiac Perfusion PET Phantom Images for Volume Extraction with Deformable Surface Models*

Anu Juslin¹, Anthonin Reilhac², Margarita Magadán-Méndez¹,
Edisson Albán¹, Jussi Tohka^{1,3}, and Ulla Ruotsalainen¹

¹ Tampere University of Technology, Institute of Signal Processing, Tampere, Finland
anu.juslin@tut.fi

² McConnell Brain Imaging Centre, Montreal Neurological Institute,
Montreal, Canada

³ Laboratory of Neuro Imaging, Division of Brain Mapping, Department of
Neurology, UCLA, School of Medicine, Los Angeles, CA, USA

Abstract. We evaluated applicability of ICA (Independent Component Analysis) for the separation of functional components from $H_2^{15}O$ PET (Positron Emission Tomography) cardiac images. The effects of varying myocardial perfusion to the separation results were investigated using a dynamic 2D numerical phantom. The effects of motion in cardiac region were studied using a dynamic 3D phantom. In this 3D phantom, the anatomy and the motion of the heart were simulated based on the MCAT (Mathematical Cardiac Torso) phantom and the image acquisition process was simulated with the PET SORTEO Monte Carlo simulator. With ICA, it was possible to separate the right and left ventricles in the all tests, even with large motion of the heart. In addition, we extracted the ventricle volumes from the ICA component images using the Deformable Surface Model based on Dual Surface Minimization (DM-DSM). In the future our aim is to use the extracted volumes for movement correction.

1 Introduction

The Positron Emission Tomography (PET) using Oxygen-15-labeled water allows for noninvasive quantification of myocardial blood flow [1]. The analysis

* This work was supported by TEKES Drug 2000 technology program, Tampere Graduate School of Information Sciences and Engineering (TISE), Graduate School of Tampere University of Technology. Anu Juslin obtained a grant from the Cultural Foundation of Pirkanmaa for this work. Jussi Tohka's work was funded by the Academy of Finland under the grants no. 204782 and 104824 and by the NIH/NCRR grant P41 RR013642, additional support was provided by the NIH Roadmap Initiative for Bioinformatics and Computational Biology U54 RR021813 funded by the NCRR, NCBC, and NIGMS.

is based on estimating the time-activity curves (TACs) of the blood pool and the myocardial tissue from the dynamic PET images. The TACs describe the time-dependent uptake of the radiopharmaceutical in tissues. However, unlike in F-18 labeled 2-fluoro-2-deoxy-D-glucose (FDG) cardiac studies it is difficult to identify the anatomical structures in $H_2^{15}O$ images, because the ^{15}O labeled water is rapidly distributed over the entire thorax region producing images with low contrast between anatomical structures. The motion of the patient and the motion of the inner structures of the thorax region are also significant problems in the analysis of functional cardiac images [2]. Because the nature of the motion in the thorax region is non-rigid and it is composed of the motion of the heart and other tissues, the detection and correction of the movement artifacts is a very complicated task. Furthermore, the varying tracer uptake and noise in dynamic images form additional challenges for the extraction of the cardiac structures.

The evaluation of the image processing procedures in cardiac PET imaging is a difficult task. However, using realistic simulations for the image acquisition process and phantom images describing the human anatomy, it is possible to evaluate the performance of image analysis algorithms. In the thorax region the motion of the involved structures has to be taken into account as well as the dynamic behaviour of the tracer in the different regions, which make the generation of the cardiac perfusion PET phantoms very demanding.

Our long term goal is to develop a procedure to correct the motion artefacts between two $H_2^{15}O$ cardiac studies of the same patient. Our novel idea is to first enhance the contrast of the cardiac perfusion PET images, so that different functional components such as ventricles and myocardium could be separated from surrounding tissues and noise. We chose the Independent Component Analysis (ICA) method [3] for this separation task. The ICA method has been previously applied to robust extraction of the input function from myocardial dog PET images [4], but has never been applied to human cardiac studies. In the second phase we will automatically extract the volumes of the ventricles and the myocardium with deformable models. The extracted volumes can then be used for the realignment of two studies.

To reach this goal we need first to assess the performance of the methods with phantom data. In this study the first goal was to analyse how well the ICA method could separate different tissues when the myocardial flow varies. The myocardial flow can differ from 40 ml/min*100g in infarcted regions up to 500 ml/min*100g during physiological stress [5]. Further on, we studied the effect of the motion of the heart on the separation of the functional components and on the automatic volume extraction with deformable surface models. In the future, we will use the extracted volumes to correct image artifacts caused by the movement of the patient.

2 Materials

Two different phantoms were generated for this study. Simple numerical 2D dynamic cardiac phantom was created for assessing the sensitivity of the ICA

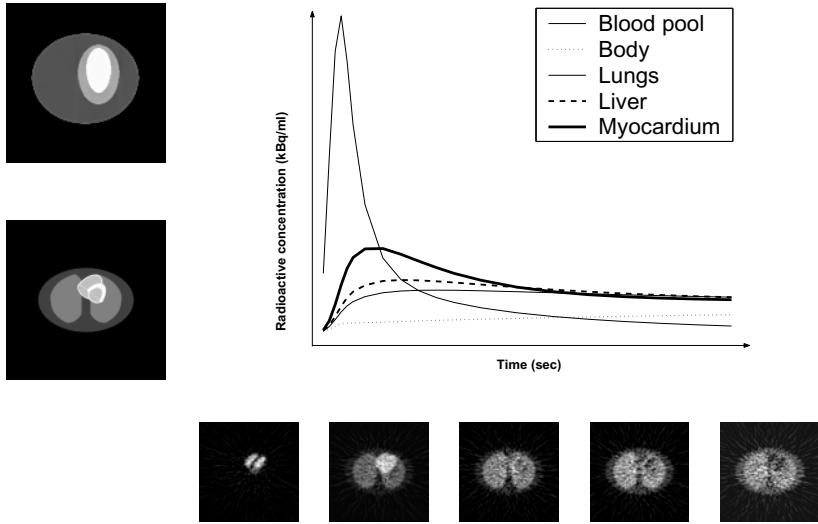


Fig. 1. In the left the anatomical geometry of the 2D phantom (Top) and the 3D phantom (Bottom). In the top right the TACs for different tissues used in the generation of the dynamic 3D cardiac perfusion PET images. In the bottom example of the simulated 3D dynamic phantom at 5 different time frames

separation of functional components with varying myocardial perfusion. In addition, with PET SORTEO, a Monte Carlo-based PET simulator [9], we generated realistic dynamic cardiac studies, using the MCAT phantom [7][8]. These simulated studies were used to investigate the impact of the heart and respiratory motions on the outcome of the separation and volume extraction processes.

The simple 2D phantom was composed of three different anatomical components: left ventricle, myocardium and body background (Fig. 1). The phantom consisted of 20 time frames (6 frames of 5 s, 6 frames of 15 s and 8 frames of 30 s) with virtual time dependent tracer distribution. We applied a measured blood TAC to calculate the tissue TACs using one block model [10]. The virtual perfusion values for the myocardium of the phantom were set from 10 ml/min*100g up to 500 ml/min*100g. For the body background the value of 5 ml/min*100g was applied in all cases. Over-dispersed Poisson noise with large variance [9] was added to the sinogram bin intensity values. The sinograms were reconstructed with filtered back projection (FBP) using Hann-filter with cut-off value 0.5.

For the evaluation of the motion effect, we generated a realistic dynamic 3D PET cardiac data set based on the MCAT phantom [7][8] using PET SORTEO software [9]. The MCAT phantom was used as an anatomical base for the phantom and the PET SORTEO software for simulating the PET dynamics with a realistic signal degradation. In our phantom we took into account 6 different anatomical structures: ventricles, atriums, myocardium, lungs, body and liver (Fig. 1). The MCAT phantom provided a possibility to simulate the motion of the heart and lungs over the time. We set the heart rate to be 60 beats per

minute and the breathing to 12 cycles per minute. The resulting 4D phantom characterizes both the physiological behaviour of the heart and lungs and the dynamic behaviour of the tracer in the involved tissues. In addition, one dynamic study without the cardiac and respiratory motions was generated corresponding to the end-diastole phase.

The tissue TACs for 3D phantom were generated similarly as in the 2D phantom. The perfusion values were set to be 75 ml/min*100g for the myocardium, 25 ml/min*100g for the lungs, 35 ml/min*100g for the liver and for the body 5 ml/min*100g (Fig. 1). The simulation of dynamic PET acquisition was carried out using Monte Carlo-based 3D PET simulator PET SORTEO [9]. This simulation tool has been dedicated to full ring PET tomography. The simulation was performed for the Ecat Exact HR+ scanner operating in 3D mode. The ^{15}O imaging protocol lasted 6 minutes with the same frame times than in the 2D phantom. The raw data was reconstructed with FBP (3DRP with Hann apodizing window and the Nyquist frequency cutoff, scatter correction, online subtraction of randoms, arc correction, normalization, and attenuation correction). This resulted in 20 time frames of 128x128x63 voxels each, whose sizes were 3.52mm x 3.52mm x 2.43mm.

3 Methods

In this study the proposed approach to extract structures of interest from $H_2^{15}\text{O}$ cardiac PET images, split into two major steps. First, the tissues of interest in the dynamic images were separated using the ICA method. Secondly, the volumes of the left and right ventricles were extracted using the DM-DSM method [12][13] from the ICA component images. The results were evaluated both visually and quantitatively. The results of automatic segmentation were compared to the ground truth by computing the Jaccard similarity coefficient [15] (also known as the Tanimoto coefficient) between the automatically segmented structures and the ground truth structures. The Jaccard value ranges from 0 for volumes that have no common voxels to 1 for volumes that are identical.

3.1 Independent Component Analysis

Our aim was to separate different tissues from dynamic cardiac perfusion data for the volume extraction. This problem was considered as a Blind Source Separation Problem. In order to solve it, we applied the ICA method on the reconstructed dynamic cardiac images. ICA is a statistical method whose goal is to represent a set of random variables as linear combinations of statistically independent component variables [3]. The ICA can be formulated to be the estimation of the following linear model for the data:

$$x = \mathbf{A}s, \quad (1)$$

where x is a random vector modelling the observations, s is a vector of the latent variables called the independent components, and \mathbf{A} is an unknown constant

matrix, called the mixing matrix. In this study, x was the vectorized form of the voxel intensity values from dynamic images and s was the vectorized form of the functional components, which we tried to separate from the dynamic images. The problem of ICA is then to estimate both the mixing matrix and the independent components using only observed mixtures.

To solve the ICA separation problem we used FastICA algorithm [14]. The FastICA algorithm is a computationally highly efficient method for performing the estimation of independent components. The resulting ICA component images were identifying those voxels to same component whose dynamic behaviour were similar. We considered that our mixture was composed of 4 different independent components. In the simple 2D phantom we knew that the amount of the source components was four (blood pool, myocardium, body and noise). In the more realistic 3D dynamic phantom we assumed that there were 4 different functional components in the field of view (blood pool, myocardium, lungs and body background including noise component).

The result of FastICA depends on the initialization of the mixing matrix \mathbf{A} . Conventionally the initialization of the FastICA has been done using a random matrix. The problem of using random initialization is that every run gives different result. For this reason we used fixed initialization to solve ICA problem with FastICA algorithm, because with fixed initialization we always end up to the same result. The initialization matrix $\mathbf{A} = (a_{ij})_{n \times m}$ was defined in the following way: $a_{ij} = 1$ if $i = j$ and otherwise $a_{ij} = 0$, n was the number of the mixtures and m was the number of the source components. PCA (Principal Component Analysis) and whitening were used as pre-processing for ICA in order to de-correlate the input data and reduce the dimensionality of data.

3.2 DM-DSM Method

For volume extraction purposes we used the DM-DSM (Deformable Model with Dual Surface Minimization) algorithm [12][13]. The surface extraction is reformulated as an energy minimization problem. The energy $E(S; I)$ of the surface S given an image I depends on the image data and the properties of the surface itself. It is a weighted sum of the internal energy penalizing surfaces that are not smooth and the external energy that couples surfaces with the image data. The total energy of the surface S is

$$E(S; I) = \lambda E_{int}(S) + (1 - \lambda) E_{ext}(S; I), \quad (2)$$

where $E_{int}(S)$ is the internal energy, $E_{ext}(S; I)$ is the external energy, and $\lambda \in [0, 1]$ is the regularization parameter controlling the tradeoff between external and internal energies.

The internal energy was based on a simple thin-plate shape model [12]. In this study, the external energy values for each voxel were derived from the ICA component images. The external energy value for each voxel was stored in look-up-table, which was called energy image. In the energy image high intensity value corresponded to surface which we were interested in. The energy images were obtained using extended 3D version of varying adaptive window size edge

detection method [16][17] to the resulting ICA component images. The starting point of the volume search was defined manually to inside of the object.

4 Results

The values of Jaccard coefficients between the reference volumes and the extracted cardiac tissue volumes are reported in Table 1. In Fig. 2, Fig. 3 and Fig. 4 the results of the ICA separation and the volume extraction are shown. We only present two resulting ICA component images, which contain the ventricles (blood pool) and the myocardium.

Table 1. The Jaccard similarity coefficients between the automatically segmented structures and the ground truth structures. The separation results of the myocardium from the 3D dynamic data were not good enough for the volume extraction

		Blood pool	Myocardium
2D phantom	myocardial flow 500 ml/min*100g	.958	.717
	myocardial flow 300 ml/min*100g	.931	.725
	myocardial flow 100 ml/min*100g	.923	.681
	myocardial flow 40 ml/min*100g	.920	.534
3D phantom	No motion	.652	
	Motion	.607	



Fig. 2. In the left the ICA separation of the blood pool and in the middle the separation of the myocardium from the 2D phantom with high myocardial flow (500 ml/min*100g). In the right the sum of the all time frame images from the original 2D phantom image

4.1 The Myocardial Flow Test

The ICA method was able to separate automatically the blood pool and myocardium even with very high myocardial blood flow values from the dynamic 2D phantom data. The separation results of the blood pool and myocardium were visually excellent. The quantitative results showed that the blood pool was extracted with very high accuracy in all cases, but the extraction of the myocardium was more dependent on the perfusion level (Table 1). We used thresholding to define the volume of the blood pool and the myocardium from the resulting ICA component images. Fig. 2. shows the result of the separation

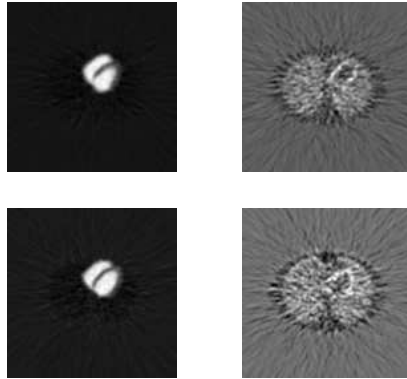


Fig. 3. The ICA separation of the functional components from the MCAT based phantom images. In the top left the blood pool and in the top right the myocardium from phantom image without motion and in the bottom left the blood pool and in the bottom right the myocardium from the phantom image with heart beating and respiratory motion

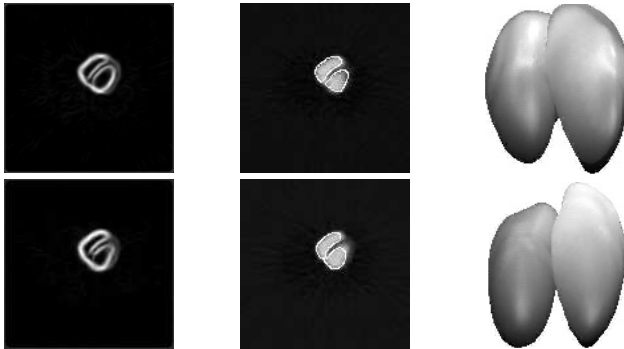


Fig. 4. The volume extraction result of the right and left ventricle from the MCAT based phantom images. In the top left the energy image of the blood pool, in the top middle the extracted volumes of the ventricles and in the top right the 3D visualization of the extracted ventricle volumes from the phantom images without the motion. In the bottom left the energy image of the blood pool, in the bottom middle the extracted volumes of the ventricles and in the bottom right the 3D visualization of the extracted volumes from phantom images with heart beating and respiratory motion. The volumes of extracted ventricles with the static phantom and the motion phantom were different (The Jaccard coefficient between these volumes was 0.7178). The surfaces have been smoothed based on [18]

with myocardial flow 500 ml/min*100g and it is compared to the sum of the time frame images. This illustrates the problem of the initial low contrast of different tissues in $H_2^{15}O$ study.

4.2 The Motion Test

The result of blood pool and myocardium separations from the MCAT based PET phantom images are shown in Fig. 3. With the static phantom and the phantom with the cardiac and respiratory motion the separation of the blood pool was visually good and it could be used for volume extraction. When looking the separation of the myocardium, we could see that the separation was more difficult and the result is not visually so good. The ICA method had problems of separating the myocardium from surrounding tissues. Especially, the separation of the myocardium from the liver with the simulated study including heart and respiratory motions was problematic. One problem with motion for separation was also that ICA caught just some phase of the heart cycle and we could not define, which phase the detected heart cycle phase was.

The separation result of myocardium was not good enough for the volume extraction. Therefore, we concentrated to extract individually the right and left ventricles from the resulting blood pool component images (cf. Fig. 3). Fig. 4 shows the result of the volume extraction with the DM-DSM method. We were able to extract the right and the left ventricles visually with good quality from the ICA component images in both cases. The extracted volumes were compared to the reference phantom corresponding to the end-diastole phase. Table 1 shows the accuracy of the methodology. With the static phantom the extracted volume corresponded more to the reference volume than with the motion phantom, because we do not know which phase of cardiac cycle was detected from the motion phantom.

5 Discussion

We have examined the applicability of the ICA method for the separation of the functional components from the dynamic cardiac perfusion images. Using ICA, it was possible to separate the ventricles (blood pool) with varying myocardial blood flow and even with large motion of the heart and lungs during the dynamic study. The separation of myocardium was more difficult task. However, it was possible to separate the myocardium with very high myocardial blood flow values, but the effect of the cardiac and respiratory motion was more problematic for the ICA method. In addition, we demonstrated the possibility to extract the volumes of the right and left ventricles from resulting ICA component images using the DM-DSM method. The extracted volumes could be used for alignment of two image sets that allows for the quantitative comparison of two studies. The DM-DSM algorithm effectively avoids local minima, which reduces its sensitivity to its initialization. Nevertheless, in this study, we needed manual interaction to generate the initialization.

In this study we created realistic phantom data for testing automatic image analysis methods in the case of dynamic $H_2^{15}O$ cardiac perfusion images. The 3D dynamic phantom contained both dynamic information of the tracer and the motion of heart and respiratory motion. It was generated using the Monte Carlo-based simulation tool and the MCAT phantom. The motion which was

included to the phantom described the extreme positions and shapes of the heart and respiratory motion during the cardiac cycle, which is not realistic in true PET imaging, where the motion in one time frame is the average motion over the frame time. The reference phantom was taken from the end-diastole phase, where the heart muscle is thinnest and the ventricles largest. This could explain the problem of separating the myocardium from surrounding tissues. The extracted volumes of the ventricles were different in static and moving case. This result implicated that it is important to construct the phantoms carefully. To achieve comparable results with patient studies also the motion needs to be taken into account. In this study, the patient movement during the acquisition was not simulated. Due to the relative short scanning time (6 minutes) in dynamic $H_2^{15}O$ cardiac perfusion study we could assumed that patient do not move.

Conventionally random matrix has been used for the initialization of the FastICA algorithm. In this study we used fixed initialization for the ICA separation. This made it possible to achieve more reproducible results in automatic way, although the used matrix may not be the optimal solution for the initialization. We have also shown that perhaps the separation should be performed on sinograms [6], because the selection of the image reconstruction method affects the result.

Our long term goal of the research is to find a procedure to correct the motion artifacts between two studies of one patient, so that both visual and quantitative analysis of the images can be performed, at least the comparison of equivalent myocardial segments. Our idea is to first enhance the contrast in $H_2^{15}O$ studies with the ICA method so that it is possible automatically extract from component images the ventricles or the myocardium for movement correction purposes. To reach this goal we evaluated the ICA method for separation of functional components from cardiac perfusion PET phantom images in this study. We studied the effect of varying myocardial flow and motion to the ICA separation results. In addition, we showed that it is possible to extract the volume of the ventricles with the DM-DSM method for movement correction purposes. In the next step we will use patient data and apply the extracted volumes for the alignment of two image sets between two or more studies of one patient.

References

1. Bergmann, SR, Herrero P, Markham J, Weinheimer CJ, Walsh MN.: *Noninvasive quantitation of myocardial blood flow in human subjects with oxygen-15-labeled water and positron emission tomography*, J Am Coll Cardiol; **14**: 639–652, (1989).
2. Ter-Pogossian, M.M., Bergmann S.R., Sobel B.E.: *Influence of Cardiac and Respiratory Motion on Tomographic Reconstructions of the Heart: Implications for quantitative Nuclear Cardiology*. J Comput Assist Tomogr, **6**(6):1148–1155, (1982).
3. Hyvärinen A., Karhunen J., Oja E.: *Independent Component Analysis*, USA, John Wiley Sons, Inc., (2001).
4. Lee, J.S., Lee D.S., Ahn, J.Y., Cheon, G.J., Kim, S-K., Yeo, J.S., Seo, K., Park, K.S., Chung, J-K., Lee, M.C.: *Blind separation of cardiac components and extraction of input function from $H_2^{15}O$ dynamic myocardial PET using Independent Component Analysis*. J Nucl Med, **42**(6): 938–943, (2001)

5. Kalliokoski, K.K., Nuutila, P., Laine, H., Luotolahti, M., Janatuinen, T., Raitakari, O.T., Takala, T.O., Knuuti, J.: *Myocardial perfusion and perfusion reserve in endurance-trained men*, Med Sci Sports Exerc 34:948-953, (2002)
6. Magadán-Méndez, M., Kivimäki, A., Ruotsalainen, U.: *ICA separations of Functional Components from Dynamic Cardiac PET data*. IEEE Nuclear Science Symposium Conference Record, **4**: 2618–2622 (2003)
7. Pretorius, P.H., Xia, W., King, M.A., Tsui, B.M.W, Lacroix, K.J.: *A mathematical model of motion of the heart for use in generating source and attenuation maps for simulating emission imaging*. Med Phys., **26**(11): 2323–2332, (1999)
8. Segars, W.P., Lalush, D.S., Tsui B.W.M.: *Modelling respiratory mechanics in the MCAT and spline based MCAT phantoms*. IEEE Trans. Nucl. Sci., **48**(1): 89–97, (2001)
9. Reilhac, A., Lartizien, C., Costes, N., Comtat, C., Evans, A.C.: *PET-SORTEO: A Monte Carlo-based simulator with high count rate capabilities*. IEEE Trans. Nucl. Sci., **51**(1): 46–52, (2004)
10. Ruotsalainen, U., Raitakari, M., Nuutila, P., Oikonen, V., Sipilä, H., Teräs, M., Knuuti, J., Bloomfield, P., Iida, H.: *Quantitative Blood Flow Measurement of Skeletal Muscle Using Oxygen-15 water and PET*. J Nucl Med **38**:314–319, (1997)
11. Furuie, S.S., Herman, G.T., Narayan, T.K., Kinahan, P.E., Karp, J.S., Lewitt, R.M., Matej, S.: *A methodology for testing of statistically significant differences between fully 3D PET reconstruction algorithms*. Phys. Med. Biol. **39**:341–354, (1994)
12. Tohka, J., Mykkänen, J.: *Deformable Mesh for Automated Surface Extraction from Noisy images*. Int. J. Image and Graphics, **4**(3):405–432, (2004)
13. Mykkänen, J., Tohka, J., Luoma, J., Ruotsalainen, U.: *Automatic Extraction of Brain Surface and Mid-sagittal plane from PET images applying deformable Models*. Technical Report of Department of Computer Sciences, University of Tampere, Finland, <http://www.cs.uta.fi/reports/r2003.html>, (2003)
14. Hyvärinen A., Oja E.: *A fast fixed-point algorithm for Independent Component Analysis*, Neural Computation, **9**(7): 1483–1492, (1997).
15. Jackson, D.A., Sommers, K.M., Harvey, H.H.: *Similarity coefficients: Measures of co-occurrence and association or simply measures of occurrence?* The American Naturalist, **133**(3):436–453, (1989)
16. Albán, E., Katkovnik, V., Egiazarian, K.: *Adaptive window size gradient estimation for image edge detection*. Proceedings of SPIE Electronic Imaging, Image Processing: Algorithms and Systems II, Santa Clara, California, USA, 54–65, (2003)
17. Albán, E., Tohka, J., Ruotsalainen U.: *Adaptive Edge Detection Based on 3D Kernel Functions for Biomedical Image Analysis*. To appear in Proceedings of SPIE Electronic Imaging, Image Processing: Algorithms and Systems IV, San Jose, California, USA, January, (2005)
18. Tohka, J.: *Surface Smoothing Based on a Sphere Shape Model*. In proc. of 6th Nordic Signal Processing Symposium, NORSIG2004, 17–20, (2004)